

Polyhedral units and network connectivity in GeO₂ glass at high pressure: An X-ray total scattering investigation

Xinguo Hong,^{1,a)} Lars Ehm,^{1,2} and Thomas S. Duffy³

¹Mineral Physics Institute, Stony Brook University, Stony Brook, New York 11794, USA

²Photon Sciences Directorate, Brookhaven National Laboratory, Upton, New York 11973, USA

³Department of Geosciences, Princeton University, Princeton, New Jersey 08544, USA

(Received 19 June 2014; accepted 16 August 2014; published online 26 August 2014)

We report a pressure-induced dense tetrahedral intermediate state via Ge–O–Ge rotation formed at 3–5 GPa and the polyhedral relations in GeO₂ glass up to 17.5 GPa using *in situ* X-ray total scattering and X-ray absorption (XAFS) techniques. It was found that the nearest-neighbor Ge–Ge correlations show a decrease reaching a minimum between 4 and 6 GPa, and exhibit negative compression behavior at 7–17.5 GPa. The Ge–Ge distance determined by XAFS shows a substantial reduction, i.e., normal compression behavior, at 7–17.5 GPa. The comparison with the theoretical $g(r)$ function for rutile-type GeO₂ (16.1 GPa) indicates that the negative compression of intermediate range order reflects the direct formation of GeO₆ octahedral units. Results of coordination number analysis show that GeO₂ glass undergoes a transition from tetrahedral GeO₄ to GeO₅ units (possibly triangular bipyramidal), and finally to octahedral GeO₆ units. The present investigation provides the structural details of the polyhedral units and their relationships in GeO₂ glass at high pressure. © 2014 AIP Publishing LLC. [<http://dx.doi.org/10.1063/1.4894103>]

Pressure-induced structural changes of the “strong” network-forming SiO₂ and GeO₂ glasses¹ have been extensively studied due to their importance in glass, materials, and geological sciences.^{2–14} Accurate determination of the pressure-dependent structure is necessary for understanding the mechanisms of network compression and corresponding property changes in SiO₂ and GeO₂ glasses.

Germanium dioxide (GeO₂) is regarded as a chemical and structural analogue of silica (SiO₂)² with similar pressure response at lower pressures due to the larger ionic radius of Ge⁴⁺. At ambient conditions SiO₂ and GeO₂ glasses are based on a relatively open arrangement of corner sharing tetrahedral units, while at high pressure the glass undergoes a transformation to a dense octahedral material.^{3,5,6}

A sharp first-order-like tetrahedral-octahedral transition in GeO₂ glass was proposed based on the rapid change of r_{Ge-O} at 7–9 GPa.⁵ Subsequently, experiments using high-energy X-ray and neutron diffraction along with molecular dynamics simulations, suggest a five-fold intermediate state ($N_{Ge}^O = 5$) is formed at 6–10 GPa and a complete octahedral glass ($N_{Ge}^O = 6$) occurs at 15 GPa.⁶ Density measurements show a plateau at 6–9 GPa in support of an intermediate state.¹⁵ There is, however, no abrupt change in r_{Ge-O} and N_{Ge}^O revealed by recent experiments using neutron diffraction,^{9,11} X-ray diffraction,¹⁰ XAFS,^{8,14} and molecular dynamics simulations.⁷ There are still some disagreements regarding the short range ordering (SRO) in GeO₂ glass.¹³

In order to bring the more distant O atoms of neighboring tetrahedral units into the first Ge–O coordination shell, significant intermediate range order (IRO) modifications are required.^{6,9–11,15} However, the nature of the cooperative mechanism between SRO and IRO remains unclear. The IRO changes in tetrahedral GeO₂ glass may be responsible for

the anelastic behavior¹⁶ and slight enhancement in density¹⁵ at 2–3 GPa. The tetrahedral-octahedral transition mechanism is yet a matter of debate.^{2,11–13}

The SRO and IRO structures of non-crystalline materials can be interpreted in detail if the partial structure functions are known. Extraction of the full sets of these pair distribution functions become possible recently using isotope-substitution neutron diffraction.¹⁷ High-energy X-ray diffraction has played a key role in unraveling the structural details of SiO₂ and GeO₂ glasses,^{3,6,10} but the structural analysis has been limited to the first Ge–O shell mainly due to the narrow Q-space coverage of $S(Q)$,^{6,10} which results in poor resolution in real space. In this paper, we propose to combine high-energy X-ray diffraction and XAFS techniques to obtain the pair distribution functions of GeO₂ glass.

GeO₂ glass was obtained by quenching GeO₂ melt annealed at 1600 °C in air for 6 h. The total x-ray scattering was conducted using a high-energy (80.865 keV) monochromatic beam at beamline X17B3, NSLS. Princeton-manufactured large-opening symmetrical diamond anvil cells (DAC) were employed for these experiments. The total scattering function, $S(Q)$, was obtained using the program PDFgetX2.¹⁸ XAFS experiments were carried out at the Ge *K*-edge of GeO₂ glass at the GeoSoilEnviroCARS beamline 13-BM-D, APS, from 10,953 to 11,747 eV, as described previously.^{13,19}

The obtained structure factors, $S(Q)$, for GeO₂ glass at pressures up to 17.5 GPa are shown in Fig. 1. The $S(Q)$ data are smooth and of good quality below 10 Å^{−1} with $S(Q)$ oscillations recognizable out to 20 Å^{−1} (Fig. 1, inset). As pressure increases to 10 GPa, the most notable change is the merging of the first sharp diffraction peak (FSDP) (1.59 Å^{−1}) with the shoulder peak (2.67 Å^{−1}) at ambient pressure.^{6,10,15}

The experimental pair distribution function $g(r)$ is obtained by Fourier transform

^{a)}Author to whom any correspondence should be addressed. Electronic addresses: xhong@bnl.gov and xinguo.hong@gmail.com

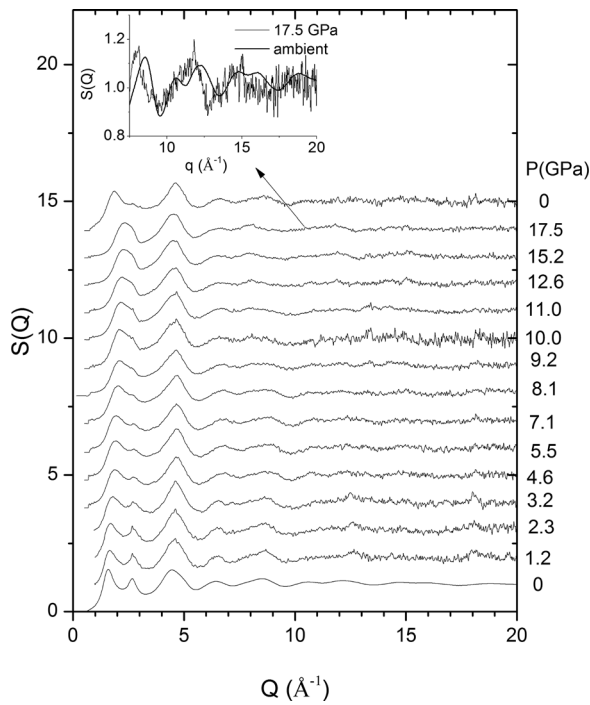


FIG. 1. Structure factor, $S(Q)$, for GeO_2 glass at different pressures. Inset compares a portion of the patterns at ambient pressure and 17.5 GPa.

$$g(r) = 1 + \frac{1}{2\pi^2\rho r} \int_0^\infty Q(S(Q) - 1)\sin(Qr)W(Q)dQ, \quad (1)$$

where ρ is the atomic number density and $W(Q)$ is a cosine window function with $W(Q) = 1$ for $Q \leq 10 \text{ \AA}^{-1}$. A reliable $g(r)$ function with few ripples can be obtained as demonstrated in experiments on fluid Hg.²⁰ If available $S(Q)$ data is below 10 \AA^{-1} , the termination at $Q_{\max} < \infty$ may introduce error in the resultant $g(r)$ as unphysical ripples, but our $S(Q)$ data extends well beyond 10 \AA^{-1} . We fixed the Q_{\max} (20 \AA^{-1}) for all datasets. To reduce the errors in the $S(Q)$ data reduction, which may result in artificial peaks in $g(r)$ at low r values,²¹ we performed a Fourier back-transform by cutting off the unphysical low $g(r)$ data below 1.2 \AA . The resulting modified $S(Q)$ is useful in the verification and error estimate for the original $S(Q)$ data.

Figure 2 shows the pair distribution function $g(r)$ calculated from the $S(Q)$ data (Fig. 1). The pressure-induced elongation of $r_{\text{Ge-O}}$ is large at 5.5–11 GPa in agreement with previous observations.^{6,9–11,15} The second peak develops a broad asymmetric profile and eventually comprises of two distances (2.79(1) \AA and 3.20(1) \AA , top panel, Fig. 2) at 17.5 GPa. The solid vertical lines show the expected peak positions in $g(r)$ calculated for rutile-type GeO_2 at 16.1 GPa²² using PDFgui.²³

Crystalline GeO_2 has two polymorphic forms at ambient conditions: the tetrahedral α -quartz-like structure (α - GeO_2) ($P3_221$)²⁴ and the octahedral rutile GeO_2 phase ($P4_2/mnm$).²⁵ α - GeO_2 has $r_{\text{Ge-O}}$ at 1.74 \AA and $r_{\text{Ge-Ge}}$ at 3.15 \AA , and is often used to simulate the structure of GeO_2 glass at low pressure.^{5,8,14} The rutile GeO_2 structure is regarded as an analogue of octahedral GeO_2 glass,^{5,8,13} containing $r_{\text{Ge-O}}$ at 1.85 \AA and two $r_{\text{Ge-Ge}}$, at 2.83 \AA and 3.35 \AA , respectively, at

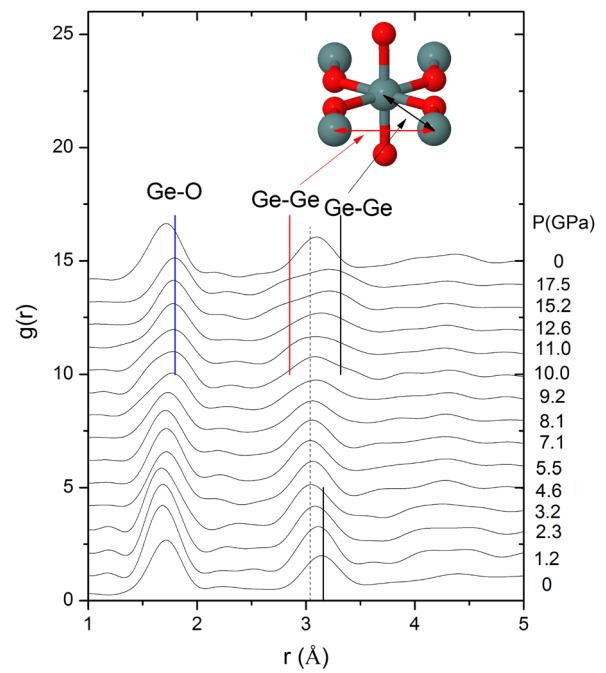


FIG. 2. Pair distribution function $g(r)$ for GeO_2 glass at different pressures. Vertical lines show the calculated Ge-O and Ge-Ge distances for α - GeO_2 (bottom) and rutile-type GeO_2 with a model (inset, O: red ball; Ge: gray ball) at 16.1 GPa.²² Vertical dashed line shows the minimum distance of Ge-Ge correlations.

16.1 GPa.²² The shoulder positions coincide with the equatorial Ge-Ge distance (Fig. 2, inset).

Theoretically, the $g(r)$ is a sum of all partial distribution $g_{ij}(r)$,

$$g(r) = \sum_{ij} w_{ij}g_{ij}(r) \quad (2)$$

here weighting factor, $w_{ij} = c_i c_j f_i(Q) f_j(Q) / [\sum c_i f_i(Q)]^2$, and c_i and $f_i(Q)$ are the type i atomic concentration and form factor, respectively. There is no easy solution for $g_{ij}(r)$.^{17,26} However, the experimental $g(r)$ shows distinct coordination shells ($< 3.5 \text{ \AA}$, Fig. 2) and can be reproduced by multiple Gaussian peaks,²¹

$$g(r) = \sum_i \frac{A_i}{\sqrt{2\pi}\sigma_i} \exp\left(-\frac{(r-r_i)^2}{2\sigma_i^2}\right), \quad (3)$$

where A_i , r_i , and σ_i denote the area, the bond length, and the mean-square distance displacement of the i th shell, respectively.

Figure 3 shows the multiple Gaussian fits to the first and second peaks of $g(r)$ functions (1.30–3.48 \AA) at pressures of 4.6, 8.1, 12.6, and 17.5 GPa, respectively. The $g(r)$ profile at 4.6 GPa can be largely reproduced by two Gaussian peaks (1.72(1) \AA and 3.06(1) \AA), which is consistent with the Ge-O and Ge-Ge distances (1.73 \AA and 3.08 \AA) of α - GeO_2 .²⁷ As pressure increases, there is considerable enhancement in the region between these two peaks. The small shoulder at 4.6 GPa grows to a third Gaussian peak found at 2.22(1) \AA at 8.1 GPa, which is shorter than previous observation of a new Ge-O distance at 2.5 \AA .⁶ At higher pressures, four Gaussian peaks are required to reproduce the

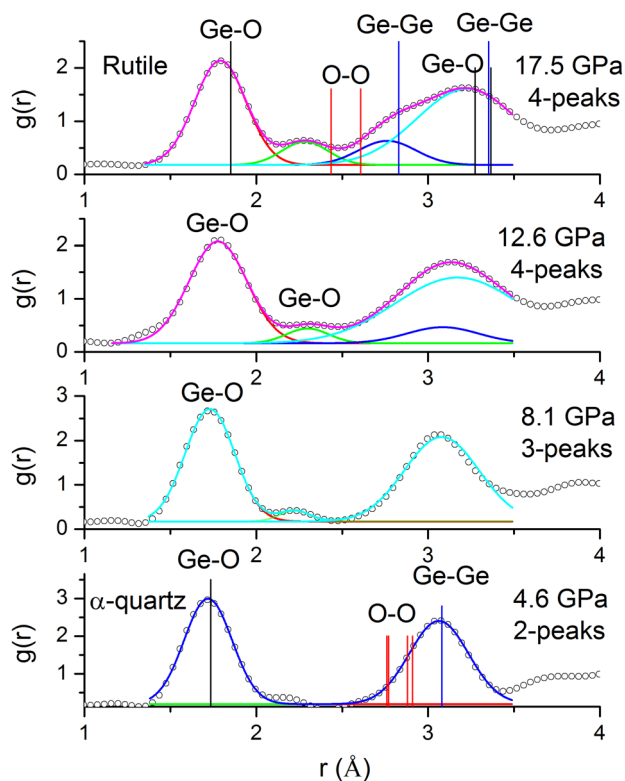


FIG. 3. Multiple Gaussian peak fits to the first and second peaks of the $g(r)$ functions for GeO_2 glass at selected pressures. Experimental data: circles; fitted data: full line; individual Gaussians: #1 red, #2 cyan, #3 green, and #4 blue. Atomic-pair distances for $\alpha\text{-GeO}_2$ (4.6 GPa, bottom) and rutile GeO_2 (16.1 GPa, top) are labeled with vertical lines (black: Ge-O; blue: Ge-Ge; and red: O-O).

$g(r)$ function. The positions of four Gaussian peaks (1.79(1), 2.28(1), 2.76(1), and 3.23(1) Å) basically coincide with the corresponding atomic pairs of rutile GeO_2 at 16.1 GPa (lines, top panel), suggesting large octahedral units formed at 17.5 GPa. Because of the large difference of atomic form factor ($Z_{\text{Ge}}/Z_{\text{O}} = 4$), the Ge-Ge correlation becomes predominant in the IRO lengths for high-energy X-ray scattering, i.e., the Ge-Ge distance can be approximately represented by the second peak position of $g(r)$.

Figure 4(a) shows the pressure evolution of the second peak position (maximum) of $g(r)$ obtained from two independent experiments. Uncertainties are evaluated by using different Q_{max} ranging from 12 \AA^{-1} to 20 \AA^{-1} . This second peak position shows a decrease that reaches a minimum at 3–6 GPa (profile, Fig. 4(b)). The pressure of 3 GPa basically agrees with the results of FSDP, density enhancement, and Raman shift at 2.5 GPa,¹⁵ and the anelastic behavior at 2–3 GPa.¹⁶ Based on the Ge-Ge distance and first Ge-O distance obtained by EXAFS,¹³ the Ge-O-Ge inter-polyhedral angle can be calculated (Fig. 4(c)). At low pressure, the Ge-O-Ge angle is close to that of $\alpha\text{-GeO}_2$, confirming the validity of the calculation. As pressure increases, GeO_2 glass shows a larger rotation than $\alpha\text{-GeO}_2$, and indicates the existence of a dense tetrahedral intermediate state.¹⁵ A relatively large reduction in Ge-O-Ge angle below 4 GPa is also evidenced from recent neutron diffraction work¹² (Fig. 4(c)).

Above 7 GPa, there is a marked increase in these IRO lengths (Fig. 4(a)). In order to understand this negative

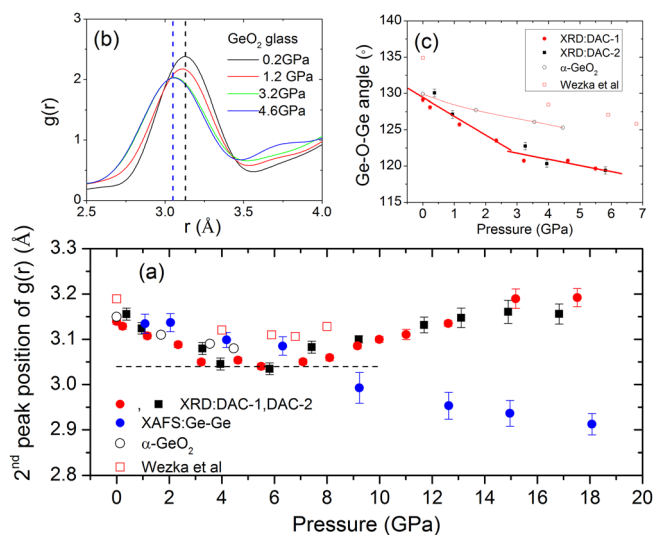


FIG. 4. (a) The pressure dependence of the second peak position of $g(r)$ function. Dashed line shows the minimum value. (b) The fast reduction of the second $g(r)$ peak occurring around 3 GPa. (c) Ge-O-Ge bond angle of inter-polyhedral bridging oxygen of tetrahedral GeO_2 glass. Lines are linear fits at [0, 2.4] and [3.2, 5.8] GPa to guide the eye. $\alpha\text{-GeO}_2$ data are calculated from Ref. 27. Ge-Ge distance and Ge-O-Ge angle determined by Wezka *et al.* (2012) is shown for comparison.¹²

compression behavior and identify the atomic type at these IRO lengths, we have conducted multi-shell fitting to the EXAFS data over a wide range (1–3 Å, no phase correction) by using $\alpha\text{-GeO}_2$ model. To get reliable fitting results, the same variables were used for all pressure steps, i.e., the amplitude, the nearest $r_{\text{Ge-O}}$, $r_{\text{Ge-Ge}}$, and two Debye-Waller factors, one for all Ge-O correlations and the other for Ge-Ge correlations, similar to the modeling of a dense octahedral glass reported previously.¹³ The obtained Ge-Ge distances (Fig. 4, blue circles) exhibit a shallower decrease at 4–6 GPa, but this is followed by increased further reduction at 7–17.5 GPa.

These two IRO lengths defined by $g(r)$ and EXAFS have contrasting compression behavior and cross over near 7 GPa (Fig. 4). In comparison with the theoretical $g(r)$ of rutile GeO_2 at 16.1 GPa (Fig. 3, top panel), the negative compression corresponds to the short Ge-Ge correlations as in the rutile GeO_2 structure, because the decrease of the Ge-Ge distance (Fig. 4, EXAFS) agrees with the formation of the distinct $g(r)$ shoulder (2.76 Å, 17.5 GPa). The elongation of main second peak (3.23 Å, Fig. 3) reflects the formation of the long Ge-Ge distance as in rutile GeO_2 (3.35 Å, 16.1 GPa). The separation of these short and long Ge-Ge distances is similar to that observed in the octahedron of rutile GeO_2 .²² This means that the formation of an octahedral glass can be directly observed by X-ray total scattering. Since $\alpha\text{-GeO}_2$ structure does not have two Ge-Ge distances, a more robust model is needed for further modeling the formation and evolution of Ge-Ge and Ge-O distances.

The mean coordination number of the Ge-O distribution is given by the integral of the radial distribution function (RDF),

$$\text{RDF}(r) = 4\pi r^2 \rho g(r). \quad (4)$$

To obtain the coordination number, N_{Ge}^{O} , from the broad RDF profiles, we integrate the first peak of RDF(r) from 1 Å to the first minimum of $g(r)$, r_{min} , which was fixed at 2.4 Å.

Figure 5 shows the pressure evolution of the mean coordination number, N_{Ge}^O , for GeO_2 glass, showing a consistent dependence for two independent experiments. The obtained N_{Ge}^O data are compared to those obtained by Guthrie *et al.*,⁶ Mei *et al.*,¹⁰ Drewitt *et al.*,⁹ and Salmon *et al.*¹¹ The present work agrees well with that of Guthrie *et al.*⁶ to 10 GPa, and we find a slightly higher coordination than Mei *et al.*¹⁰ at a given pressure, but our data are higher than those obtained by neutron diffraction.¹¹ The discrepancy between the neutron and x-ray diffraction values may come from the Q dependent atomic form factors.²⁶

Below 5 GPa, the Ge atoms remain largely four-fold coordinated. The predominant structural change is the approach of neighboring tetrahedral GeO_4 motifs via the bending of Ge–O–Ge angles of corner-sharing tetrahedral units (Fig. 4). As pressure increases, the value of N_{Ge}^O increases to 4.7–5.1 at 6–10 GPa, where the GeO_2 glass could be in a pentahedral intermediate state.^{6,28} For the tetrahedral–octahedral transition, there are two sites in the octahedron that can adopt the additional O atoms, either axial or equatorial. At 7–10 GPa, the Ge–Ge distance is still much longer than that of rutile GeO_2 (2.85 Å, Fig. 2), implying that the addition of O atom should not take place in the equatorial plane of the octahedron. In the range of 7–10 GPa, where N_{Ge}^O is steady, the local structure of Ge atom may remain in penta-coordinated units, waiting for the further approach of neighboring polyhedral units, which is evidenced by the rapid decrease of Ge–Ge distance (Fig. 4). At higher pressures, there is a second rapid change of N_{Ge}^O from 4.8 to 5.6 at 10–13 GPa (Fig. 5). This is followed by a steady increase of the N_{Ge}^O values to 5.9 at 17.5 GPa. At 17.5 GPa, the r_{Ge-Ge} determined by EXAFS and Gaussian fitting of $g(r)$ are 2.91 Å and 2.76 Å, respectively, which generally agree well with the short Ge–Ge distance of rutile GeO_2 at 2.85 Å.²² These equatorial Ge atoms are tightly associated with the equatorial octahedral O atoms (inset, Fig. 2). This illustrates that the last O atom is added into the equatorial plane of the GeO_6 octahedron. In other words, the entrance of the first O atom occupies the axial position of GeO_6

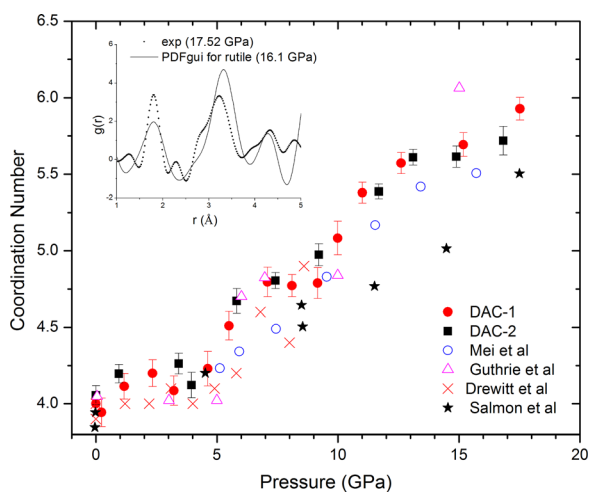


FIG. 5. The pressure evolution of the mean coordination number N_{Ge}^O for GeO_2 glass. The results are compared to the results of previous X-ray and neutron diffraction experiments.^{6,9–11} Inset shows the comparison of $g(r)$ between glassy and rutile GeO_2 .

octahedron, forming a triangular bipyramid GeO_5 unit. Wezka *et al.* reported predominant distorted square pyramidal GeO_5 units,¹² which should not be excluded because of the highly disordered GeO_5 units at 10 GPa.¹³

To cross-check the completion of octahedral units at 17.5 GPa, the $g(r)$ function of rutile GeO_2 at 16.1 GPa²² was evaluated, showing good consistency with GeO_2 glass (inset, Fig. 5). The results of PDF calculations, $g(r)$ analysis (Fig. 3), and coordination number (Fig. 5) are consistent with each other, indicating the roughly completion of octahedral units in GeO_2 glass at 17.5 GPa.

The major results illustrated in Fig. 5 indicate a compression mechanism of GeO_2 glass from tetrahedral GeO_4 , to possibly triangular bipyramid GeO_5 , and to octahedral GeO_6 units upon the capture of the first and second O atoms into the first Ge–O coordination shell. The tetrahedral–octahedral transition in GeO_2 glass is largely completed at 17.5 GPa, which is in good agreement with results of Guthrie *et al.*⁶ and recent XAFS studies.¹³

We have observed the formation of a precursor dense tetrahedral intermediate state at 3–5 GPa in GeO_2 glass, and also observed the direct formation of octahedral GeO_2 glass at 12.6–17.5 GPa. The GeO_2 glass undergoes a compression pathway from tetrahedral GeO_4 , GeO_5 (possibly triangular bipyramid), and to octahedral GeO_6 units. The present investigation enriches the knowledge of polyhedral units and their pressure evolution in the strong network-forming GeO_2 glass.

We thank D. Weidner for useful discussions, and M. Newville, X. M. Yu, Z. Zhong, L. P. Huang, and S. Lin for assistance. This research was partially supported by COMPRES under NSF Cooperative Agreement EAR 11-57758.

¹C. A. Angell, *Science* **267** (5206), 1924 (1995).

²M. Micoulaut, L. Cormier, and G. S. Henderson, *J. Phys.: Condens. Matter* **18** (45), R753 (2006).

³C. Meade, R. J. Hemley, and H. K. Mao, *Phys. Rev. Lett.* **69**(9), 1387 (1992).

⁴A. C. Wright, *J. Non-Cryst. Solids* **179**, 84 (1994); G. Lelong, L. Cormier, G. Ferlat, V. Giordano, G. S. Henderson, A. Shukla, and G. Calas, *Phys. Rev. B* **85**(13), 134202 (2012).

⁵J. P. Itie, A. Polian, G. Calas, J. Petiau, A. Fontaine, and H. Tolentino, *Phys. Rev. Lett.* **63**(4), 398 (1989).

⁶M. Guthrie, C. A. Tulk, C. J. Benmore, J. Xu, J. L. Yarger, D. D. Klug, J. S. Tse, H. K. Mao, and R. J. Hemley, *Phys. Rev. Lett.* **93**(11), 115502 (2004).

⁷K. V. Shanavas, N. Garg, and S. M. Sharma, *Phys. Rev. B* **73**(9), 094120 (2006).

⁸M. Baldini, G. Aquilanti, H. K. Mao, W. Yang, G. Shen, S. Pascarelli, and W. L. Mao, *Phys. Rev. B* **81**(2), 024201 (2010).

⁹J. W. E. Drewitt, P. S. Salmon, A. C. Barnes, S. Klotz, H. E. Fischer, and W. A. Crichton, *Phys. Rev. B* **81**(1), 014202 (2010).

¹⁰Q. Mei, S. Sinogeikin, G. Shen, S. Amin, C. J. Benmore, and K. Ding, *Phys. Rev. B* **81**(17), 174113 (2010).

¹¹P. S. Salmon, J. W. E. Drewitt, D. A. J. Whittaker, A. Zeidler, K. Wezka, C. L. Bull, M. G. Tucker, M. C. Wilding, M. Guthrie, and D. Marrocchelli, *J. Phys.: Condens. Matter* **24**(41), 415102 (2012).

¹²K. Wezka, P. S. Salmon, A. Zeidler, D. A. J. Whittaker, J. W. E. Drewitt, S. Klotz, H. E. Fischer, and D. Marrocchelli, *J. Phys.: Condens. Matter* **24**(50), 502101 (2012).

¹³X. Hong, M. Newville, T. S. Duffy, S. R. Sutton, and M. L. Rivers, *J. Phys.: Condens. Matter* **26**(3), 035104 (2014).

¹⁴M. Vaccari, G. Aquilanti, S. Pascarelli, and O. Mathon, *J. Phys.: Condens. Matter* **21**(14), 145403 (2009).

- ¹⁵X. Hong, G. Shen, V. B. Prakapenka, M. Newville, M. L. Rivers, and S. R. Sutton, *Phys. Rev. B* **75**(10), 104201 (2007).
- ¹⁶O. B. Tsiok, V. V. Brazhkin, A. G. Lyapin, and L. G. Khvostantsev, *Phys. Rev. Lett.* **80**(5), 999 (1998).
- ¹⁷P. S. Salmon, A. C. Barnes, R. A. Martin, and G. J. Cuello, *Phys. Rev. Lett.* **96**(23), 235502 (2006).
- ¹⁸X. Qiu, J. W. Thompson, and S. J. L. Billinge, *J. Appl. Crystallogr.* **37**(4), 678 (2004).
- ¹⁹X. Hong, M. Newville, V. B. Prakapenka, M. L. Rivers, and S. R. Sutton, *Rev. Sci. Instrum.* **80**(7), 073908 (2009).
- ²⁰X. Hong, M. Inui, T. Matsusaka, D. Ishikawa, M. H. Kazi, and K. Tamura, *J. Non-Cryst. Solids* **312–314**, 284 (2002).
- ²¹M. Inui, X. Hong, and K. Tamura, *Phys. Rev. B* **68**(9), 094108 (2003).
- ²²J. Haines, J. M. Lager, C. Chateau, and A. S. Pereira, *Phys. Chem. Miner.* **27**(8), 575 (2000).
- ²³C. L. Farrow, P. Juhas, J. W. Liu, D. Bryndin, E. S. Božin, J. Bloch, T. Proffen, and S. J. L. Billinge, *J. Phys.: Condens. Matter* **19**(33), 335219 (2007).
- ²⁴G. S. Smith and P. B. Isaacs, *Acta Crystallographica* **17**(7), 842 (1964).
- ²⁵W. H. Baur and A. A. Khan, *Acta Crystallographica B* **27**(11), 2133 (1971).
- ²⁶A. Zeidler, J. W. E. Drewitt, P. S. Salmon, A. C. Barnes, W. A. Crichton, S. Klotz, H. E. Fischer, C. J. Benmore, S. Ramos, and A. C. Hannon, *J. Phys.: Condens. Matter* **21**(47), 474217 (2009).
- ²⁷T. Yamanaka and K. Ogata, *J. Appl. Crystallogr.* **24**(2), 111 (1991).
- ²⁸J. Badro, D. M. Teter, R. T. Downs, P. Gillet, R. J. Hemley, and J.-L. Barrat, *Phys. Rev. B* **56**(10), 5797 (1997).